Green Flame Retardancy: Biomass-Based Treatment for Poplar Wood

Igor Wachter
Slovak University of Technology in Bratislava
Veronika Kvorková
Slovak University of Technology in Bratislava
Tomáš Štefko
tomas.stefko@stuba.sk

Slovak University of Technology in Bratislava
Peter Rantuch
Slovak University of Technology in Bratislava
Jozef Martinka
Slovak University of Technology in Bratislava
Chia-Feng Lin
Luleå University of Technology
Lenka Blinová
Slovak University of Technology in Bratislava

Research Article

Keywords: ammonium phytate, flame retardant fixation, multifunctional wood modification, poplar, wood upcycling

Posted Date: December 17th, 2025

DOI: https://doi.org/10.21203/rs.3.rs-8327322/v1

Additional Declarations: No competing interests reported.

Version of Record: A version of this preprint was published at European Journal of Wood and Wood Products on April 13th, 2026. See the published version at https://doi.org/10.1007/s00107-

026-02406-4.

GREEN FLAME RETARDANCY: BIOMASS-BASED TREATMENT FOR POPLAR WOOD

Igor Wachter[1], Veronika Kvorková[1], Tomáš Štefko[1*], Peter Rantuch[1], Jozef Martinka[1], Chia-Feng Lin[2], Lenka Blinová[1]

[1]Institute of Integrated Safety, Faculty of Materials Science and Technology in Trnava, Slovak University of Technology in Bratislava, 91724 Trnava, Slovakia

[2]Department of Engineering Sciences and Mathematics, Wood Science and Engineering, Luleå University of Technology, 97187 Luleå, Sweden

[*]Corresponding author: tomas.stefko@stuba.sk

ABSTRACT

Poplar wood (*Populus alba* L.) was modified using a fully bio-based treatment that combined furfuryl alcohol (FA) and ammonium phytate (AMP), catalysed by phosphoric acid. The in-situ polymerization created a cross-linked poly(furfuryl alcohol) matrix that effectively immobilized AMP within the wood structure. The treatment increased weight percent gain to 21.7% and density from 0.394 to 0.499 g cm^{-3}. FTIR and SEM confirmed the uniform incorporation of FA and AMP in both cell walls and lumina. The modified wood showed a limiting oxygen index of 28% compared to 18% for untreated wood, produced up to 35.7% char at 800 °C, and self-extinguished rapidly during flame exposure. Fire tests demonstrated substantial reductions in total heat release, carbon monoxide, and smoke production, along with a six-fold increase in residual mass. Water uptake decreased by 38%, while Shore D and Janka hardness increased by 12% and 18%, respectively. Importantly, leaching resistance exceeded 91%, confirming durable fixation of the flame-retardant system. These synergistic improvements in fire safety, moisture resistance, and mechanical properties highlight a sustainable approach for producing high-performance, flame-retardant lignocellulosic materials from low-value poplar.

KEYWORDS: ammonium phytate, flame retardant fixation, multifunctional wood modification, poplar, wood upcycling

INTRODUCTION

Wood, a renewable form of lignocellulosic biomass, is a promising alternative to fossil fuels. With an exceptional strength-to-weight ratio and the ability to sequester carbon, it's a valuable material for construction and decorative applications (Sangregorio et al. 2020; Zhang et al. 2021). The rapid growth of poplar makes it an especially attractive resource. However, poplar's inherent flammability is a major limitation. Enhancing its performance through chemical modification is crucial for expanding its use.

Chemical modification alters wood properties by changing the composition of its cell walls or modifying its structure (Rowell 1983). The hydroxyl groups in wood's cell walls make it

prone to swelling and shrinking with changes in moisture and also contribute to its flammability (Jones et al. 2020; Dong et al. 2023).

To improve fire safety, wood is often treated with flame retardants containing elements like halogens, phosphorus, nitrogen, or boron. These are applied through methods like impregnation and coating (Lowden and Hull 2013; Xie et al. 2013). While halogenated compounds are effective, they raise environmental and health concerns and are being phased out (Page et al. 2023).

Phosphorus-based flame retardants are gaining favour due to their lower toxicity and effectiveness in cellulose-based materials (Abou-okeil et al. 2013). They work primarily by promoting char formation, which slows combustion. A significant challenge, however, is that many flame retardants can leach from the wood, diminishing their long-term effectiveness. This has led to a focus on developing sustainable, bio-based impregnation solutions with high leach resistivity (Lin et al. 2021a, b; Wu et al. 2023).

Phytic acid (PA), a natural phosphorus source, is an ideal candidate for a bio-based flame retardant. It is non-toxic, inexpensive, and works by promoting carbonization and scavenging flammable radicals when heated (Cheng et al. 2016; Gao et al. 2019). When combined with nitrogen-rich compounds like urea, it forms ammonium phytate (AMP), which offers a powerful synergistic flame-retardant effect. In this system, phosphorus promotes char formation while nitrogen produces non-combustible gases (Li et al. 2022, 2024; Song et al. 2022; Qin et al. 2023).

The issue of leaching from these small-molecule flame retardants can be solved by embedding them within a polymerized resin matrix. Furfuryl alcohol (FA) is an environmentally friendly chemical derived from agricultural biomass (Yao et al. 2017). Its water-soluble nature allows it to penetrate wood cell walls, where it polymerizes in-situ into poly(furfuryl alcohol) (PFA). This improves the wood's dimensional stability and resistance to biodegradation (Ehmcke et al. 2020). However, PFA itself can contribute to flame spread and toxic smoke release during combustion (Gaefke et al. 2007; Zhang et al. 2020). This highlights the need for flame-retardant furfurylated wood that also provides heat insulation and smoke suppression.

Previous studies have explored combining these approaches. Liangliang Zhang et al., (2022) used a boron/phosphorus system to catalyse FA polymerization while providing fire resistance. Similarly, in other research the fire performance of pine wood with an ammonium phytate-based flame retardant was improved (Zhang et al. 2023). More recently, a study by (Xie et al. 2024) demonstrated that the in-situ polymerization of FA and ammonium phytate (AMP) could enhance flame retardancy, dimensional stability, and leach resistance.

This study tests the central hypothesis that the in-situ polymerization of a low-concentration furfuryl alcohol (15 wt%) and ammonium phytate (4 wt%) solution, uniquely catalysed by phosphoric acid, will form a stable, cross-linked matrix that physically entraps the AMP flame retardant. We predict this system will create a durable, multifunctional material with synergistically enhanced properties. The novelty lies in using phosphoric acid not only as an efficient catalyst for FA polymerization but also as a supplementary phosphorus source to

enhance char formation, thereby creating a highly effective and leach-resistant fire-retardant system at lower treatment concentrations than previously reported.

To validate this hypothesis, we impregnated poplar wood with the FA+AMP+H_3PO_4 formulation and subjected it to a comprehensive analysis of its fire, mechanical, and physical properties, with a specific focus on performance before and after a rigorous 14-day leaching protocol.

MATERIAL AND METHODS

Materials

Poplar veneer (*Populus alba* L.) with an average air-dry density of 0.440 ± 0.20 g cm^{-3} was obtained from JAF HOLZ Slovakia, Ltd. (Slovakia). Specimens were cut exclusively from sapwood, free of visible defects. The material was conditioned outdoors under natural climatic conditions for several months before being processed. Prior to chemical modification, all samples were oven-dried at 100 °C until both mass and dimensions stabilized. For testing, two sets of specimens were prepared: larger blocks (100 × 100 × 20 mm^3; longitudinal (L) × radial (R) × tangential (T)) used in cone calorimetry, hardness, and colour measurements, and smaller cubes (20 × 20 × 20 mm^3; L × T × R) for FTIR spectroscopy, thermogravimetric analysis (TGA), and leaching experiments. Details regarding the number of replicates, sample sizes, and associated test methods are listed in Table 1.

Table 1 Wood specimen preparation for tests

Specimen Size (mm^3)	Test Type	Replicates
100 x 100 x 20	Cone calorimetry	12
	Leaching	12
	Hardness	16
	Colourimetry	12
	Water uptake	12
20 x 20 x 20	TGA	3
	FTIR analysis	3
100 x 10 x 4	LOI	10

Phytic acid (PA, $C_6H_{18}O_{24}P_6$, 50 wt% in water), urea (CH_4N_2O, 99%), furfuryl alcohol (FA, $C_5H_6O_2$, purity ≥ 98.0%), phosphoric acid (H_3PO_4, 85 %) was purchased from CENTRALCHEM, Ltd., Slovakia.

Ammonium phytate synthesis

A solution was prepared by dissolving urea (43.2 g, 0.72 mol) and phytic acid (PA) (79.2 g, 0.12 mol) in deionized water (36 g) until fully homogenized. The ratio of the amount of substances was determined based on previous studies (Feng et al. 2017; Zuo et al. 2023; Xie et al. 2024). PA solution was heated in a three-necked bottle at 110 °C by an oil bath for 8 hours. A stirrer and reflux equipment were installed for achieving a homogeneous heat

distribution and preventing reagents from drying out. Upon cooling to ambient temperature, the reaction yielded a brown-tinted ammonium phytate (AMP) solution with a pH of approximately 6.

Modified poplar wood preparation

Poplar specimens were cut into various dimensions according to standard requirements, and defect-free pieces with an oven-dried density of approximately 0.36–0.40 g/cm³ were chosen for modification. The aqueous impregnation solution was formulated by combining 15 wt% FA with 4 wt% AMP, and its pH was adjusted to around 2 using phosphoric acid (denoted as FA+AMP-W). The samples were impregnated through the following process: first subjected to a vacuum of 0.3 kPa for 2 h, followed by 16 h of treatment under normal atmospheric pressure. After impregnation, excess solution was removed by wiping with a cloth. The treated specimens were then wrapped in aluminium foil and heat-cured at 130 °C for 24 h to ensure complete reaction of FA and AMP. Subsequent gradual drying was applied until the samples reached a constant weight. For comparison, two sets of control specimens were prepared using the same procedure but with different impregnation solutions: one containing 4 wt% AMP adjusted to pH $\approx$ 2 with phosphoric acid (AMP-W), and the other containing 15 wt% FA adjusted to pH $\approx$ 2 (FA-W).

Chemical and physical characterization

According to Liu et al., (2021), the weight percent gain (WPG) of the modified poplar samples was calculated as:

$$WPG(\%) = \frac{w_f - w_0}{w_0} \times 100\%$$

, where w_0 is initial weight of oven-dry sample, w_f is the oven-dry weight of sample after impregnation. Additionally, the density was determined according to the GB/T 1927.5–2021 standard. Calculated values of the WPG and densities are shown in Table 3.

Fourier-transform infrared spectroscopy

Fourier Transform Infrared (FTIR) spectra were acquired using an Agilent Technologies Varian FT-IR Spectrometer 660 (USA) equipped with a PIKE Technologies GladiATR accessory (USA). Spectra were collected in the 4000–400 cm^{-1} range with a resolution of $2cm^{-1}$ and averaged over 256 scans. The final spectra were corrected for background air absorbance. Each sample type (W, AMP-W, FA-W, and FA+AMP-W) was measured at five distinct locations (n=5), and the reported spectrum represents the average of these five measurements.

Scanning electron microscopy

The morphology of the samples was observed with high resolution scanning electron microscope JEOL JSM 7600F in secondary electron imaging (LEI). Following parameters were used: U = 10 kV, I = 2 nA, WD = 15 mm. Prior observation, the samples were coated with an amorphous carbon (10 – 20 nm).

Colourimetry

Colour measurements were performed with a NR200 Precision Colorimeter (Threenh Technology Co., Ltd., Shenzhen, China) using an Φ8 mm aperture, CIE L*a*b* colour space, and D65 light source. Each test specimen was measured 5 times, and the colour change from raw sample was calculated from:

$$\Delta E_t = \sqrt{(L_1 - L_0)^2 + (a_1 - a_0)^2 + (b_1 - b_0)^2}$$

where ΔE_t is the total colour difference at time t; L_1 is the value of coordinate indicating lightness after the test; L_0 is the initial value of coordinate indicating lightness, a_1 is the value of coordinate position between red and green after the test; a_0 is the initial value of coordinate position between red and green; b_1 is the value of coordinate position between yellow and blue after the test; b_0 is the initial value of coordinate position between yellow and blue.

Hardness

To evaluate the hardness of the modified poplar wood samples, two distinct methods were employed. Shore D hardness was assessed using a Sauter HD Digital Shore D Hardness Tester (Sauter GmbH, Balingen, Germany), in accordance with the Shore Hardness Test ISO 48-4 (ASTM D2240) standard. Additionally, Janka hardness was measured according to ASTM D143. For both measurements, the hardness was tested perpendicular to the grain of the samples to ensure consistent and accurate data collection.

Leaching test and water uptake

Leaching tests were performed in five replicates according to EN 84 (1997), with specimens' vacuum-treated for 20 min and leached in water replaced ten times over 14 days. After this period, the surface of the samples was dried, and the samples were weighed to determine the water uptake, according to the equation:

$$WU = \frac{m_{wu} - m_1}{m_1} \times 100\%$$

where WU is water uptake (%); m_1 is the weight of the dry-oven sample after the corresponding solution impregnation (g); m_{wu} is wet weight of the sample after leaching test (g).

Subsequently, the leached specimens were oven-dried at 103 °C, before measuring the dry mass. In this experiment the leach retention (LR; the weight of impregnation substance retained in the sample after leaching test) was calculated from:

$$LR = \left(1 - \frac{m_1 - m_f}{m_1 - m_0}\right) \times 100\%$$

where LR is leach retention (%); m_1 is the weight of the dry-oven sample after the corresponding solution impregnation (g); m_0 is initial the dry-oven weight of the sample (g); m_f is the weight of dry oven sample after the leaching test.

Thermogravimetric analysis

Thermogravimetric analysis (TGA) analysis was performed to assess the thermal degradation of various wood samples. The study included raw wood (RW), furfuryl alcohol-treated wood (FA-W), AMP-treated wood (AMP-W), and wood treated with both furfuryl alcohol and AMP (FA+AMP-W). Measurements were taken on samples before and after a leaching process.

Measurements were performed using a Netsch STA 449 F5 Jupiter instrument. Each sample was prepared by crushing and drying at 103 °C to a constant weight, with a final weight of approximately 5 mg. The analysis was carried out under a inert (N_2) atmosphere (60 mL/min) with a heating rate of 10 °C/min, from 35 °C to 800 °C.

Fire performance test

The fire hazards of the materials were determined using a cone calorimeter, following the ISO 5660-1:2015 standard (International Organization for Standardization 2015). This standard specifies the procedure for assessing the heat release rate, smoke production, and mass loss rate of materials.

Samples were exposed to an external radiant heat flux of 50 ± 0.5 kW m^{-2}. Three individual replicates of each material type (RW, AMP-W, FA-W, and FA+AMP-W) were tested for their fire performance. The measurements were conducted both before and after a leaching procedure to evaluate the durability of the fire performance properties.

For each material, four replicate measurements were used to calculate sample densities. These values, along with the ambient measurement conditions, are presented in Table 2.

Table 2 Sample densities and ambient testing conditions for raw wood (RW); furfuryl alcohol-treated wood (FA-W); ammonium phytate-treated wood (AMP-W); furfuryl alcohol and ammonium phytate-treated wood (FA+AMP-W), before (NL) and after (L) the leaching procedure

Sample	Density [g cm^{-3}]	Ambient temperature [°C]	Ambient pressure [kPa]	Air humidity [%]
RW /NL	0.384 ± 0.001	26.5 ± 0.7	100.21 ± 0.28	20.00 ± 1.41
RW /L	0.387 ± 0.008	25.3 ± 1.2	100.96 ± 1.21	23.67 ± 4.62
AMP-W /NL	0.436± 0.022	25.0 ± 1.0	100.90 ± 1.20	24.00 ± 4.36
AMP-W /L	0.427 ± 0.006	24.5 ± 0.7	100.32 ± 0.88	22.00 ± 3.60
FA-W /NL	0.475 ± 0.007	25.0 ± 1.0	100.86 ± 1.23	23.67 ± 1.23
FA-W /L	0.472 ± 0.009	25.1 ± 1.2	100.85 ± 0.49	20.25 ± 1.50
FA+AMP-W /NL	0.508 ± 0.020	24.3 ± 0.6	100.24 ± 1.19	26.67 ± 4.93
FA+AMP-W /L	0.480 ± 0.044	24.0 ± 1.0	100.91 ± 0.87	21.30 ± 4.10

Values are given as mean ± standard deviation

Limiting oxygen index

The Limiting Oxygen Index (LOI) test was conducted to evaluate the flammability of the samples. This standard method determines the minimum concentration of oxygen, expressed as a percentage, required in a mixture with nitrogen to support the sustained combustion of

a material. The LOI tests were performed in accordance with ISO 4589-2:2017 standards using a customized LOI apparatus (International Organization for Standardization 2017). Each sample was cut into rectangular specimens measuring 100 mm x 10 mm x 4 mm. The specimens were held vertically in a glass chimney, and a mixture of oxygen and nitrogen was introduced from the bottom. An external flame was used to ignite the top of the specimen. The oxygen concentration was then systematically adjusted to find the minimum value at which the sample continued to burn for at least 3 minutes, or over a length of 50 mm, after the external flame was removed. This procedure was repeated for each sample type to ensure reproducibility.

Flame test

The flame retardancy of the wood samples was qualitatively assessed using an in-lab direct flame test (Xie et al. 2024). Samples were secured in a stainless-steel clamp and positioned 10 cm from the tip of a propane torch. After ignition, the samples were exposed to the flame, and the time required for the flame to burn through the sample was recorded. The flame spread process was documented using a video camera, with simultaneous still photographs taken (0 seconds, 10 seconds and after flame-out).

Statistical analysis

Statistical significance of differences in the measured values among the investigated wood modifications was evaluated using Duncan's multiple range test at a significance level of $\alpha = 0.05$. Results of Duncan's test are indicated by letter indexes in the figures. Because listing all Duncan test outcomes for the tables would be excessively long in the main text, the complete pairwise comparison results are provided in Supplementary Material A. Duncan's coefficients were calculated using StatSoft Statistica 10 software.

RESULTS AND DISCUSSION

Chemical and physical characterization of unmodified and modified poplar wood

The weight percent gain (WPG) and density data in Table 3 demonstrate the effectiveness of the modification process, showing how the uptake of impregnation solutions alters the poplar wood's density. The lowest WPG was achieved in AMP-W samples, namely 9.55 ± 0.88, while the average density of the samples changed from 376 g cm^{-3} to 416 g cm^{-3}. WPG of FA-W and FA+AMP-W reached similar. The data suggest that FA and AMP successfully permeated the wood structure, contributing to an enhanced density.

Table 3 Impregnation formulation, weight percent gain (WPG) [%], and initial (ρ_0) [g cm^{-3}] and after-impregnation density (ρ_1) [g cm^{-3}] of raw wood (RW); furfuryl alcohol-treated wood (FA-W); ammonium phytate-treated wood (AMP-W); furfuryl alcohol and ammonium phytate-treated wood (FA+AMP-W)

Samples	Impregnation solution	WPG [%]	ρ_0 [g cm^{-3}]	ρ_1 [g cm^{-3}]
RW	–	–	0.382 ± 0.019	–
FA-W	15wt% FA; pH adjusted to ≈2 with H_3PO_4	20.31 ± 1.74	0.364 ± 0.007	0.456 ± 0.003
AMP-W	4wt% AMP; pH adjusted to ≈2 with H_3PO_4	9.55 ± 0.88	0.376 ± 0.009	0.417 ± 0.011
FA+AMP-W	15wt% FA; 4wt% AMP; pH adjusted to ≈2 with H_3PO_4	21.72 ± 1.61	0.394 ± 0.015	0.499 0.013

Values are given as mean ± standard deviation

Fourier-transform infrared spectroscopy

FTIR-ATR spectroscopy was employed to identify the functional groups present in wood and to evaluate the chemical changes resulting from modification (Fig. 1). In the spectrum of unmodified wood (RW), characteristic absorption bands were observed at 3309 cm^{-1}, corresponding to O–H stretching vibrations of cellulosic hydroxyl groups (Yang et al. 2022b; Zhang et al. 2022b; Ni et al. 2024; Xie et al. 2024; Brisebois et al. 2025). The band at 1719 cm^{-1} was attributed to unconjugated C=O stretching in xylan, a hemicellulose component (Yang et al. 2022b). Bands at 1591, 1506, and 1421 cm^{-1} corresponded to aromatic skeletal vibrations in lignin (Liu et al. 2022; Zhang et al. 2022b; Ni et al. 2024; Brisebois et al. 2025), while the band at 1451 cm^{-1} represented C–H deformation coupled with aromatic skeletal vibration (Zhang et al. 2022b). Further peaks were detected at 1364 cm^{-1} (C–H deformation in cellulose and hemicellulose) (Zhang et al. 2022b; Brisebois et al. 2025), 1152 cm^{-1} (C–O–C antisymmetric bridge stretching in cellulose and hemicellulose) (Zhang et al. 2022b; Xie et al. 2024), 1102 cm^{-1} (C–O stretching in hemicellulose) (Brisebois et al. 2025), and 1019 cm^{-1} (C–O stretching mainly in cellulose) (Yang et al. 2022a).

Following furfurylation, notable changes were observed in the regions around 3300, 1731, 1589, 1508, 1455, 1419, and 1363 cm^{-1} in the spectra of FA-modified wood (FA-W and FA+AMP-W). The broad band near 3300 cm^{-1}, assigned to O–H stretching of wood polymers, exhibited reduced intensity in the modified samples compared with untreated wood. This decrease indicates that the hydrophobic poly(furfuryl alcohol) (PFA) polymer occupied nanopores within the cell wall, thereby reducing the number of accessible hydroxyl groups and decreasing wood hygroscopicity (Zhang et al. 2022b). The unconjugated C=O stretching band of xylan shifted slightly to lower wavenumbers (from 1731 to 1700 cm^{-1}), accompanied by a decrease in intensity and peak broadening. Such changes are attributed to the incorporation of furfural resin, characterized by a C=O stretching vibration of γ-diketone groups near 1724 cm^{-1} arising from opened furan rings (Yang et al. 2022b; Zhang et al. 2022b). A decrease in the band at 1363 cm^{-1} was also observed, likely resulting from acid hydrolysis of polysaccharides during modification. The reduction in intensity of aromatic skeletal vibration

bands at 1589, 1508, 1455, and 1419 cm^{-1} suggests interactions between lignin and furfuryl alcohol during the polycondensation process. These results are consistent with the findings reported by Zhang et al. (2022b).

After the addition of ammonium phytate, further spectral variations were evident in the regions 1510–1770, 1240, and 1030–1200 cm^{-1} in both AMP-W and FA+AMP-W samples. The modifications in the 1510–1770 cm^{-1} region correspond to O–P–O stretching vibrations (Liu et al. 2018; Xie et al. 2024). The peak near 1240 cm^{-1} was assigned to P=O stretching (Feng et al. 2017; Liu et al. 2018), while the peaks between 1030 and 1200 cm^{-1} were ascribed to P=O and P–O–C vibrations of ammonium phytate (Feng et al. 2017; Fang et al. 2022). These phosphate-related peaks were more pronounced in AMP-containing samples compared with unmodified wood. Moreover, characteristic absorption bands at 3220 and 1400 cm^{-1} were detected in AMP-W and FA+AMP-W, corresponding to the stretching and bending vibrations of NH_4^+ ions (Liu et al. 2018; Xie et al. 2024). The absence of clearly distinguishable NH_4^+ bands in some spectra may result from overlap with the strong, broad O–H and C–H vibrations intrinsic to the wood matrix.

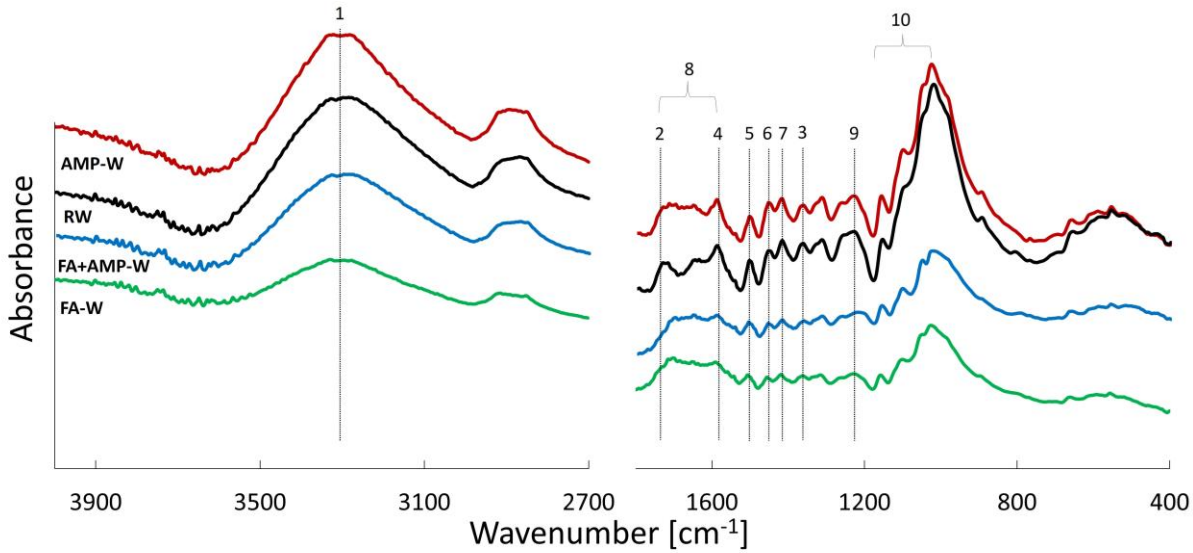

Fig. 1. FTIR analysis of the raw wood (RW); furfuryl alcohol-treated wood (FA-W); ammonium phytate-treated wood (AMP-W); furfuryl alcohol and ammonium phytate-treated wood (FA+AMP-W)

Scanning electron microscopy

Scanning electron microscopy (SEM) was performed to analyse the microstructure and morphology of the wood samples (Fig. 2). The images demonstrate significant differences between the treatments. Compared to raw wood (RW), the wood treated with both furfuryl alcohol and AMP (FA+AMP-W, images c and g) shows thickened vessel walls and more filled intercellular spaces. This indicates the reagents effectively permeated the wood. In contrast, AMP-treated wood (AMP-W, images b and f) displays distinct deposits within the vessels, indicating poor integration and potential for dislodgement. The wood treated with furfuryl alcohol alone (FA-W, images d and h) exhibits well-filled cell lumens, with the resin showing

strong adhesion to the vessel walls. These observations support the conclusion that the phosphoric acid-catalysed in-situ polymerization of FA effectively fixed AMP within the wood, which is consistent with other analytical findings.

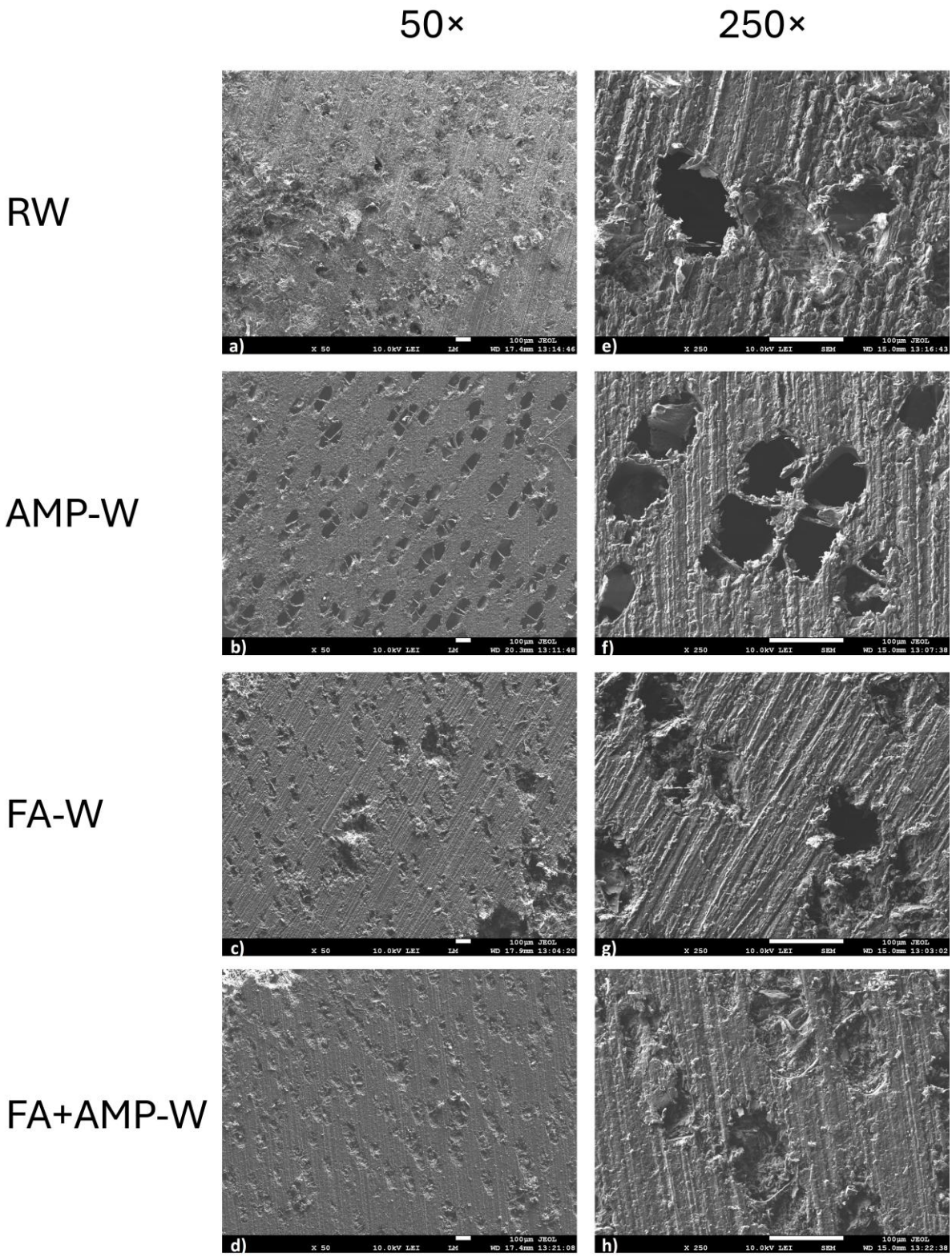

Fig. 2. Scanning electron micrographs (SEM) images of the prepared wood samples in cross-section. The images show the surface morphology of: (a, e) raw wood (RW); (b, f) AMP-treated wood (AMP-W); (c, g) furfuryl

alcohol-treated wood (FA-W); and (d, h) furfuryl alcohol and ammonium phytate-treated wood (FA+AMP-W). Figures a – d captured at 50× magnification; e – h captured at 250× magnification.

Colour measurements

Colorimetric analysis using the CIELab model was performed to quantify colour changes and identify premium wood species with similar aesthetic qualities to the modified wood. Figure 3 demonstrates a progressive shift towards a yellowish-brown hue and increased darkening in the following order: AMP-W, FA+AMP-W, and FA-W. The CIELab analysis revealed that FA+AMP-W exhibited a colour profile closely resembling that of commercially available African blackwood *(Dalbergia melanoxylon,* Guill. & Perr*.)* a species prized for its attractive appearance and diverse applications.

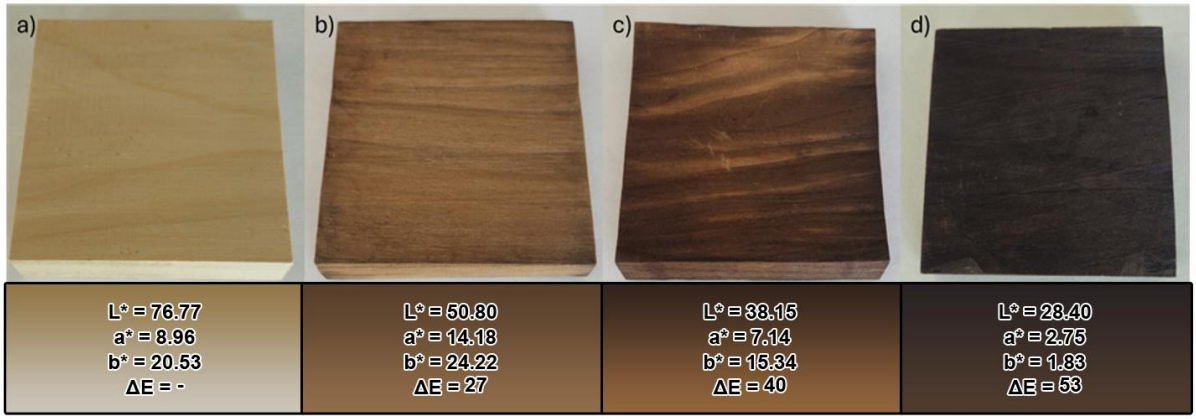

Fig. 3. Photographs of wood samples: a) raw wood (RW); b) AMP-treated wood (AMP-W); c) furfuryl alcohol-treated wood (FA-W); d) furfuryl alcohol and AMP-treated wood (FA+AMP-W). The table below the images provides the CIELAB colour parameters for each sample: L∗ (lightness), a∗ (green-red axis), b∗ (blue-yellow axis), and ΔE (total colour difference). The ΔE values are calculated relative to the raw wood (RW) sample.

Hardness

The hardness of modified wood is critical for its intended applications and the results of both Shore D and Janka hardness measurements, are summarized in Fig. **4**. The raw wood (RW) samples served as the baseline, and the reached values (50 Shore D – 50; Janka – 18 N mm^{-2}) are consistent with other works (Candan et al. 2013; Zhou et al. 2019). The AMP-W samples showed no significant change in Shore D and Janka hardness compared to RW. In contrast, the FA-W samples demonstrated a notable increase in both Shore D (7.1 %) and Janka (18.0 %) hardness. The most prevalent increase in Shore D hardness (12.2 %) was observed for the FA+AMP-W samples. Janka hardness reached similar values as FA-W (18 %). The incorporation of FA significantly improves the hardness of wood, as evidenced by the increase in both Shore D and Janka hardness values. The combination of FA and AMP further enhances Shore D hardness, suggesting a synergistic effect between the two additives. However, the addition of AMP alone does not appear to have a significant impact on either Shore D or Janka hardness. The significant increase in Shore D hardness for FA+AMP-W

compared to FA-W is likely due to the formation of phosphate-based crosslinks or interactions from AMP, which increase microscale rigidity and resistance to localized indentation. However, these chemical interactions do not significantly increase bulk compressive strength, which governs Janka hardness. Therefore, Janka values plateau at the level achieved by FA alone.

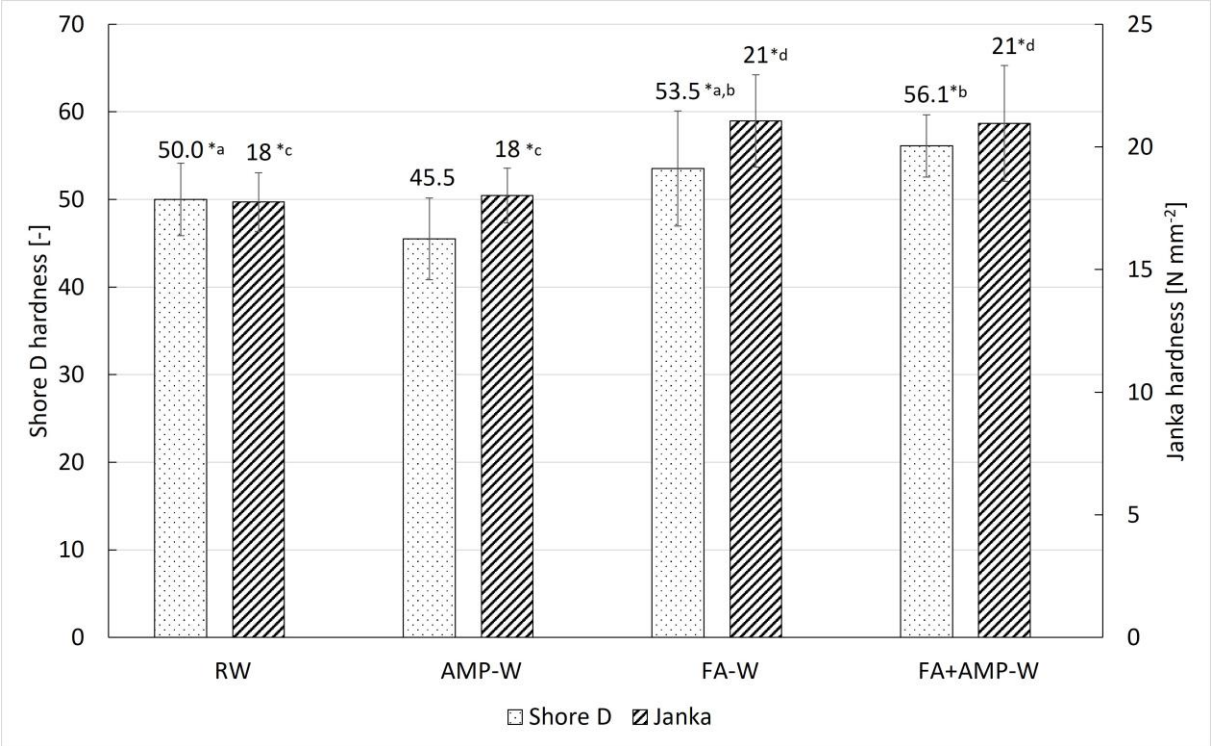

Fig. 4. Shore D and Janka hardness of raw wood (RW); furfuryl alcohol-treated wood (FA-W); ammonium phytate-treated wood (AMP-W); and furfuryl alcohol and ammonium phytate-treated wood (FA+AMP-W). Superscript *a, *b, *c, and *d indicate that there is no statistically significant difference between the corresponding values (based on Duncan's multiple range test).

Water uptake and leaching test

The two-week water uptake (WU) measurements revealed a clear trend among the tested wood specimens (Fig. 5). The raw wood (RW) exhibited the highest water uptake at 170%. Treatment with ammonium phytate alone (AMP-W) resulted in a modest reduction to 157%, while treatment with furfuryl alcohol (FA-W) caused a more substantial decrease to 117%. The most effective treatment was the combination of furfuryl alcohol and ammonium phytate (FA+AMP-W), which showed the lowest water uptake at 106%, representing a significant improvement over the other treatments and a reduction of nearly 38% compared to the RW.

Water uptake analysis confirmed that furfuryl alcohol (FA) significantly enhances the dimensional stability of wood by reducing its hygroscopicity. This effect is attributed to the in-situ polymerization of FA within the cell wall, which fills nanopores and limits the availability of hydrophilic sorption sites (Thygesen et al. 2010; Sun et al. 2022). Ammonium phytate (AMP) alone showed only a minor reduction in water uptake; however, when

combined with FA, a synergistic effect was observed. The FA+AMP-treated samples exhibited the lowest water uptake, suggesting improved moisture resistance due to combined polymer network formation and phosphate-based interactions.

This is supported by Xie et al. (2024), who demonstrated that poplar wood modified via in situ polymerization of FA and AMP exhibited exceptional water resistance and dimensional stability, alongside significantly improved flame retardant properties. These results indicate that dual modification with FA and AMP effectively enhances the wood's resistance to moisture, making it suitable for applications in humid or variable environments. Kong et al. (2018) demonstrated that combining furfuryl alcohol with ammonium dihydrogen phosphate (a simple inorganic phosphate) reduced water uptake and improved dimensional stability. While ammonium phytate differs structurally, its similar phosphorus content may lead to analogous synergistic effects when combined with FA, particularly in reducing wood hygroscopicity and improving water resistance.

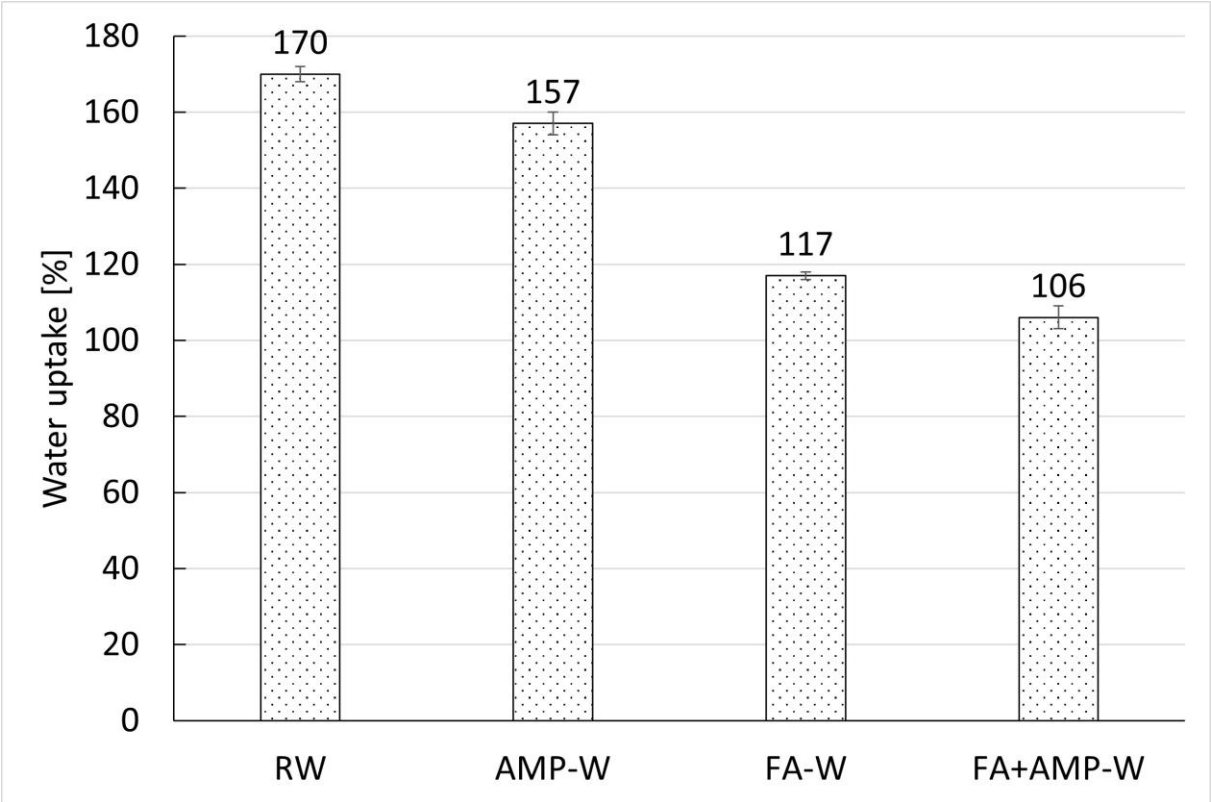

Fig. 5. Two-week water uptake (WU) of raw wood (RW); furfuryl alcohol-treated wood (FA-W); ammonium phytate-treated wood (AMP-W); and furfuryl alcohol and ammonium phytate-treated wood (FA+AMP-W). All differences between the corresponding values are statistically significant (based on Duncan's multiple range test).

Leach retention (LR) was used to assess the effectiveness of PFA and AMP fixation within the wood (Fig. 6). The results indicate that furfuryl alcohol (FA) plays a critical role in enhancing the retention and leaching resistance of water-based additives in modified poplar wood.

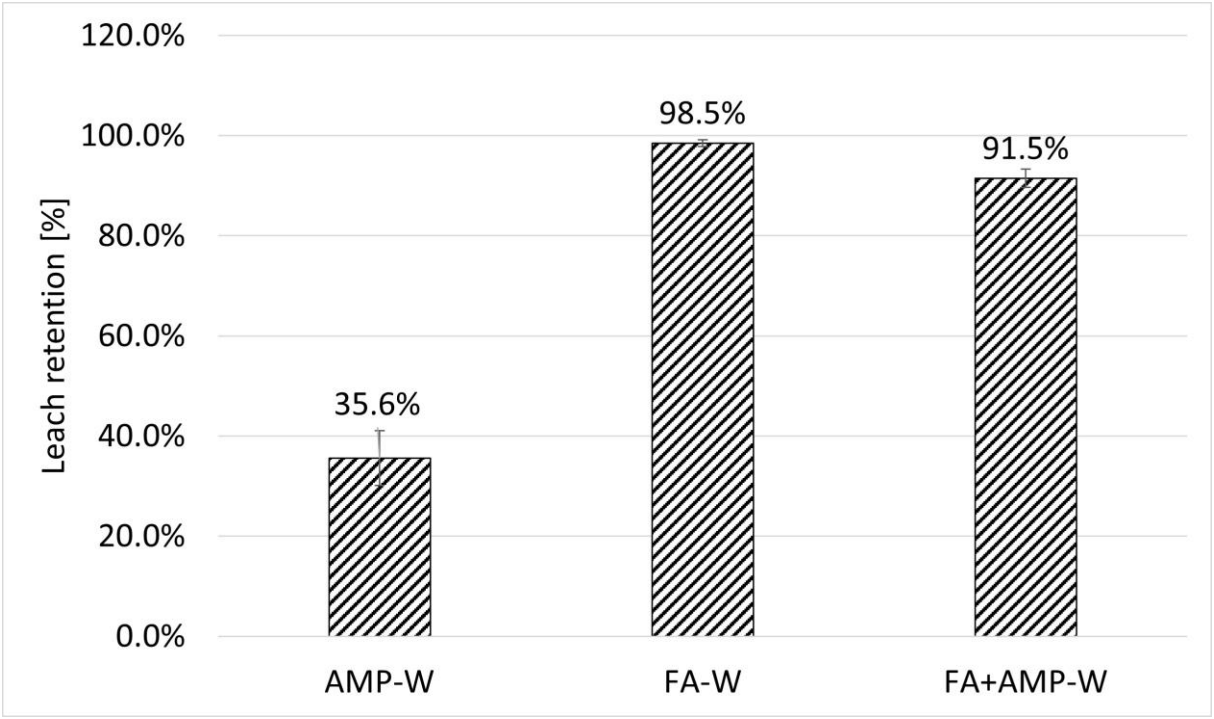

Fig. 6. Leach retention of raw wood (RW); furfuryl alcohol-treated wood (FA-W); ammonium phytate-treated wood (AMP-W); and furfuryl alcohol and ammonium phytate-treated wood (FA+AMP-W). All differences between the corresponding values are statistically significant (based on Duncan's multiple range test).

In the AMP-W sample, where only ammonium phytate (AMP) was used, leaching retention was markedly low (35.6%), suggesting that AMP alone lacks sufficient affinity or binding strength with the wood matrix. This observation aligns with existing literature indicating that phosphorus-based flame retardants like AMP are prone to leaching when not fixed within a polymeric or crosslinked system, thereby limiting their long-term effectiveness (Rowell 2005; Hörold 2014)

In contrast, FA-W samples exhibited a near-complete leaching retention (98.5%), reflecting the highly effective in-situ polymerization of furfuryl alcohol within the cell walls. The polymerization of FA is known to be strongly acid-catalysed, and the use of phosphoric acid to adjust the solution pH to approximately 2 would have significantly accelerated the polymerization process. Acidic conditions, particularly at low pH, promote both the formation of furfuryl alcohol carbocations and the condensation reactions necessary to form the poly(furfuryl alcohol) network (Iroegbu and Ray 2024). This leads to a more complete and uniform curing within the wood structure, contributing to the excellent retention and dimensional stability observed in furfurylated wood (Mubarok et al. 2023).

The FA+AMP-W combination treatment achieved a similarly high leaching retention of 91.5 %, suggesting that FA effectively enhances the fixation of AMP. This is likely due to both physical entrapment of AMP within the furfurylated matrix and potential chemical interactions between AMP and the polymerizing FA. Similarly, the research by Xie et al., (2024) confirms this principle. In their work, wood treated with only AMP also leached almost completely, while the combination of FA and AMP significantly improved retention. This alignment reinforces the conclusion that the FA polymer network is crucial for enhancing the

durability and long-term effectiveness of water-based additives in wood. While both studies robustly support the strategy of using in-situ FA polymerization to fix water-soluble flame retardants in wood, the choice of catalyst and the concentration of the treatment solution are critical factors that significantly influence the final leach resistance of the modified material. The use of phosphoric acid as a catalyst appears to be particularly effective, leading to exceptionally high retention rates and thus a more durable, long-lasting treatment. In addition, phosphoric acid not only functions as a catalyst but also serves as a phosphorus source that can synergize with AMP in enhancing the flame-retardant properties of the final material. The use of a mild, non-volatile acid like phosphoric acid is advantageous over stronger mineral acids (e.g., HCl or H_2SO_4), as it avoids excessive wood degradation while still enabling efficient FA polymerization (Zuo et al. 2023). The slight decrease in retention compared to FA alone could reflect either a minor disruption in FA polymerization due to the presence of AMP or partial leaching of AMP that was not fully immobilized.

Collectively, these results confirm that furfurylation under acidic conditions substantially improves additive retention during leaching and that combining FA with AMP results in a multifunctional treatment that enhances both durability and flame retardancy. The synergistic behaviour is largely attributed to the acid-catalysed formation of a stable polymer matrix that incorporates AMP within the wood structure, thereby reducing its leachability and improving performance.

Thermal stability

To fully understand the flame-retardant mechanism of ammonium phytate (AMP) on wood, a thermogravimetric (TGA) analysis of the pure AMP material was first performed. This preliminary analysis allowed for the characterization of its thermal decomposition pathway and the identification of key degradation products, such as phosphoric acid, which is critical for its char-forming effect. Based on the thermogravimetric (TG) analysis, the decomposition of the prepared AMP occurs in four main stages, as shown in Fig. **7**:

- Stage 1: Mass loss of approximately 3.5% occurs between 80 °C and 122 °C, with a maximum degradation rate observed at 114 °C.
- Stage 2: This is the most significant stage, occurring between 122 °C and 277 °C. The sample loses nearly 50% of its mass, with a peak in the derivative thermogravimetric (DTG) curve at 170 °C.
- Stage 3: Between 277 °C and 412 °C, the sample loses about 10% of its mass, and the maximum rate of mass loss is at 313 °C.
- Stage 4: A mass loss of 19% occurs in the temperature range of 412 °C to 615 °C, with the DTG peak occurring at 547 °C.

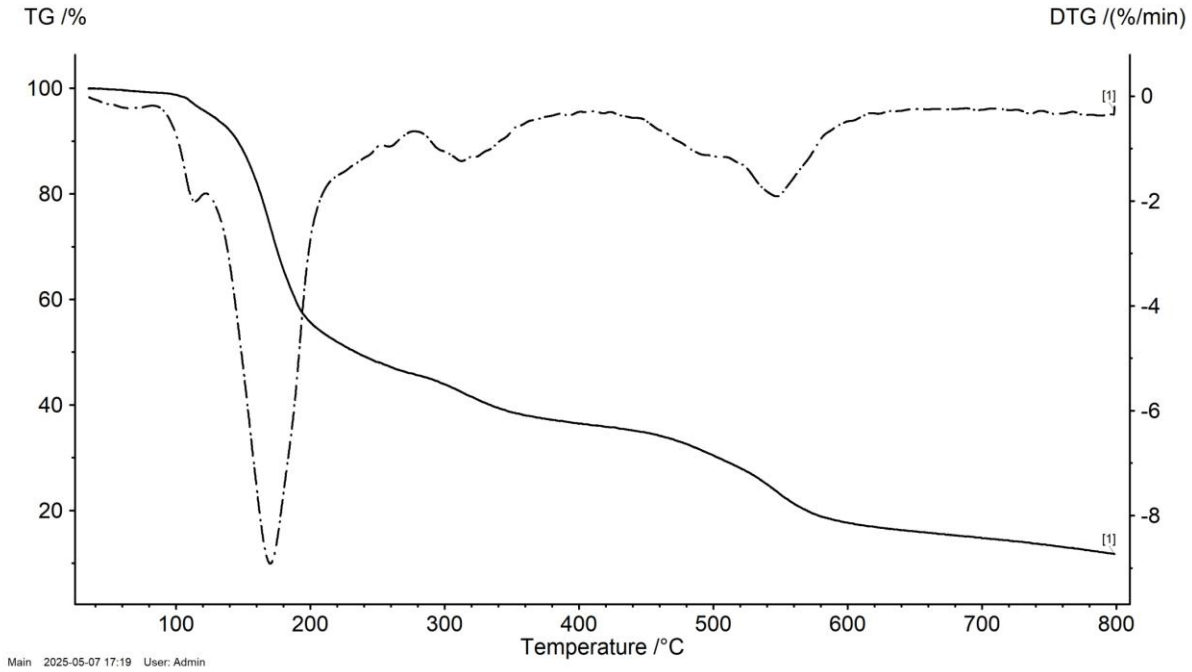

Fig. 7. Thermogravimetric (TG) and derivative thermogravimetric (DTG) curves of ammonium phytate (AMP).

This decomposition profile is consistent with and expands upon findings in existing literature. Zhang et al. (2023) identified three main decomposition stages for AMP. They reported that the first stage (102 °C – 232 °C) involves the decomposition of ammonium phytate and urea, releasing phosphoric acid and ammonia. While their subsequent two stages of decomposition were similar to those observed for phytic acid, their AMP analysis showed a broader DTG peak between 230 °C and 400 °C. They attributed this broader peak to secondary reactions of urea by-products. Similarly, Fang et al. (2022) stated that AMP decomposes to produce ammonia (at approximately 200 °C) and phosphate, which then decomposes to phosphoric acid. This formation of phosphoric acid is also supported by Feng et al. (2017), who further noted that some $-P-O-NH^{4+}$ groups remain in the charred residue of materials treated with AMP.

To evaluate the effectiveness of the treatments, thermogravimetric analysis (TGA) was conducted on all wood samples, comparing the thermal behaviour of the non-leached (Fig. 8) and leached (Fig. 9) samples. All the findings are presented in the Table 4.

Table 4 Results of thermogravimetric analysis for non-leached (NL) and leached (L) samples of raw wood (RW); furfuryl alcohol-treated wood (FA-W); ammonium phytate-treated wood (AMP-W); furfuryl alcohol and ammonium phytate-treated wood (FA+AMP-W)

Sample	Leaching	1st step			2nd step			Residue at 800 °C [%]
		Temperature range [°C]	t_{pDTG} [°C]	Δm [%]	Temperature range [°C]	t_{pDTG} [°C]	Δm [%]	
RW	NL	35 – 115	–	1.6	203 – 385	352.2	73.1	11.6
	L	35 – 116	–	0.6	206 – 402	370.0	77.7	11.8
FA–W	NL	35 – 114	–	0.5	177 – 388	353.1	65.7	21.2
	L	35 – 90	–	0.6	181 – 407	344.4	64.4	22.4
AMP–W	NL	35 – 113	–	0.9	183 – 325	299.5	51.7	26.4
	L	35 – 115	–	1.1	178 – 398	365.2	75.4	11.9
FA+AMP–W	NL	35 – 92	–	0.8	159 – 296	278.4	31.5	35.7
	L	35 – 90	–	0.9	168 – 317	288.5	37.2	30.0

t_{pDTG} – peak temperature of the derivative thermogravimetric (DTG) curve; Δm – mass loss; raw wood (RW); furfuryl alcohol-treated wood (FA-W); ammonium phytate-treated wood (AMP-W); furfuryl alcohol and ammonium phytate-treated wood (FA+AMP-W)

The TG curves of the non-leached samples are shown in Fig. **8**. All samples showed a minor initial mass loss on the TG curve at temperatures up to 115 °C. This phenomenon is commonly observed in lignocellulosic materials and is typically attributed to the evaporation of moisture (Li et al. 2019; Vahedi et al. 2022; Zhang et al. 2022a). Given that the materials were pre-dried at 103 °C before the analysis, this initial mass loss likely corresponds to moisture adsorbed during sample preparation.

In the second stage of mass loss, a significant difference is observed between samples containing AMP and those without it. The addition of AMP resulted in an acceleration of sample decomposition, shifting the DTG peak from approximately 350 °C to around 290 °C. Concurrently, the total mass loss was less pronounced, leading to a much higher char residue.

This phenomenon is caused by phosphoric acid, which redirects the thermal decomposition of cellulose. According to Zhang et al., (2023), the acid facilitates the production of a higher yield of char and less flammable gases at reduced temperatures.

This effect is attributed to the influence of phosphoric acid, which alters the pyrolysis pathway of cellulose toward the production of less combustible volatiles and more char at lower temperatures.

The presence of furfuryl alcohol (FA) also had an evident impact, leading to a more significant formation of char residue. This outcome is consistent with prior work in the field, such as C. Lin et al. (2021) and (Acosta et al. 2022).

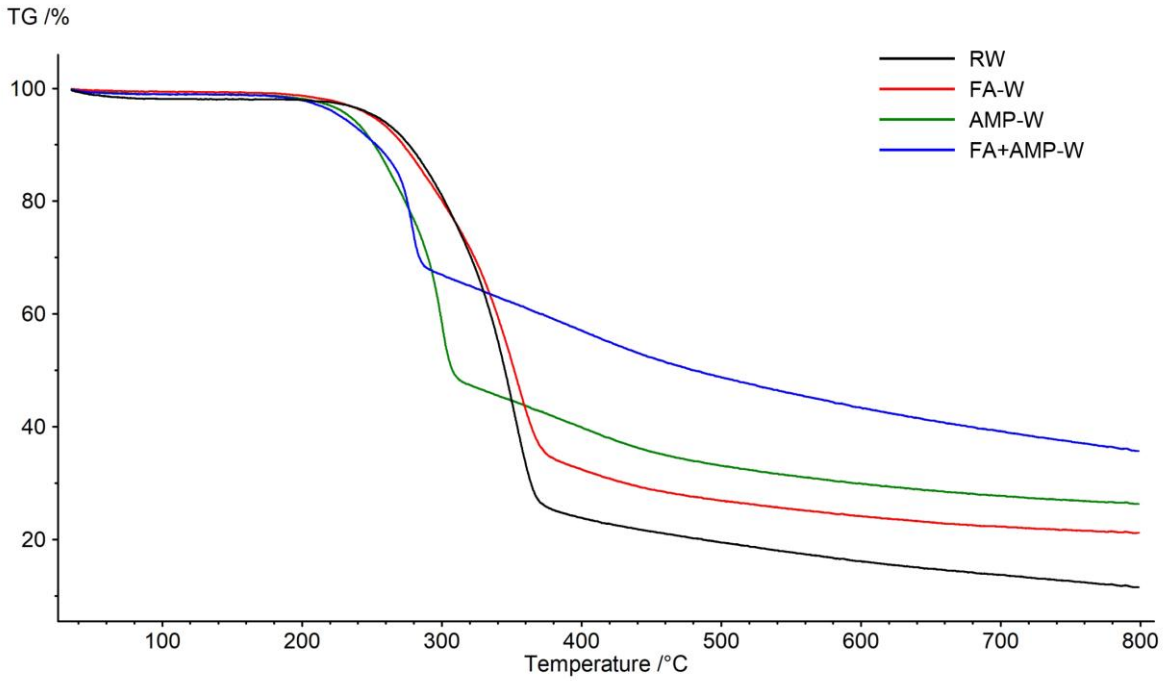

Fig. 8. Thermogravimetric (TG) curves of the non-leached raw wood (RW); furfuryl alcohol-treated wood (FA-W); ammonium phytate-treated wood (AMP-W); furfuryl alcohol and ammonium phytate-treated wood (FA+AMP-W)

The TG curves for the leached samples (Fig. 9) show a very slight initial mass loss, similar to the non-leached samples, which is attributed to moisture removal. The progression of the TG curve for the raw wood (RW) sample is identical for both leached and non-leached wood.

However, a significant change is observed in the behaviour of the AMP-W sample, where its TG curve is practically identical to that of the RW sample. This suggests that almost all the AMP was leached out, as its effect on the thermal stability of the sample was no longer evident.

Conversely, the FA-W samples behaved nearly identically regardless of whether they were subjected to leaching. In the case of FA+AMP-W, only a minor change was observed after leaching. This indicates that a significant portion of the AMP was not removed, suggesting that the furfurylation process helped to prevent its leaching from the wood.

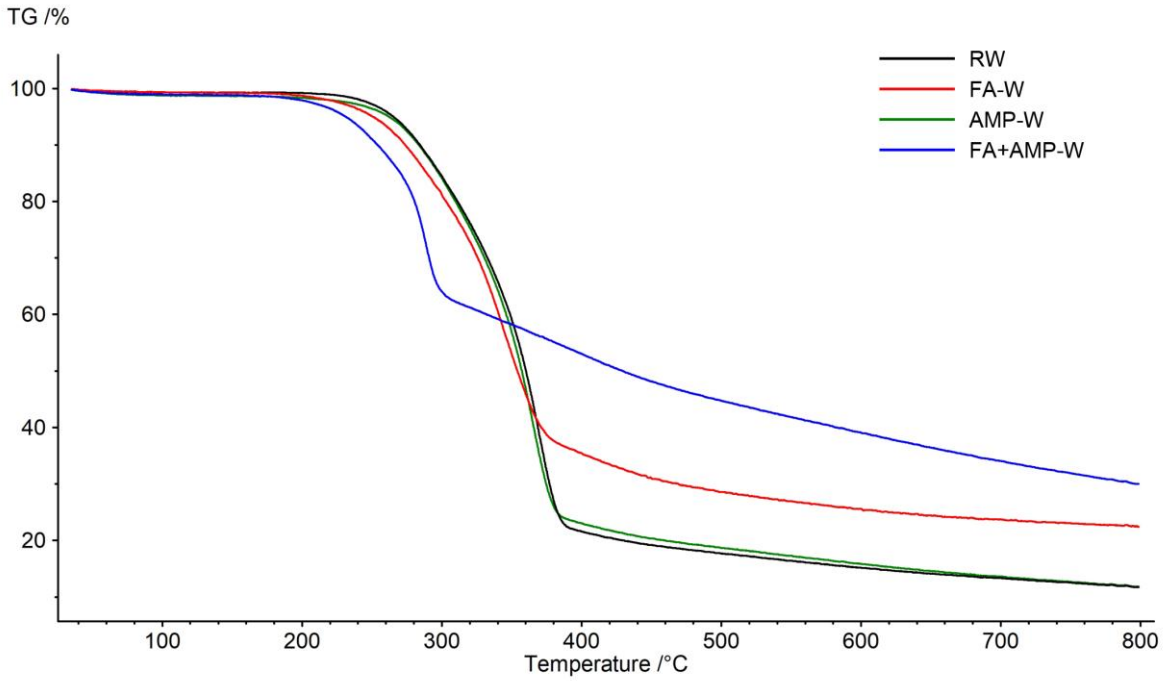

Fig. 9. Thermogravimetric (TG) curves of the raw wood (RW); furfuryl alcohol-treated wood (FA-W); ammonium phytate-treated wood (AMP-W); furfuryl alcohol and ammonium phytate-treated wood (FA+AMP-W)

Fire performance test

Cone calorimetry was used for a comprehensive evaluation of the fire performance of raw and treated poplar wood, with results summarized in Table 5 and Fig. **10**. The analysis focused on comparing the performance between different sample types (RW, AMP-W, FA-W, and FA+AMP-W) and assessing the durability of the treatments by testing samples before (NL) and after (L) a rigorous 14-day leaching procedure.

Table 5 Fire performance of raw wood (RW); ammonium phytate-treated wood (AMP-W); furfuryl alcohol-treated wood (FA-W); furfuryl alcohol and ammonium phytate-treated wood (FA+AMP-W)

Sample [-]	RW		AMP-W		FA-W		FA+AMP-W	
Leaching [-]	**NL**	**L**	**NL**	**L**	**NL**	**L**	**NL**	**L**
TTI [s]	7 ± 1	7 ± 1	7 ± 1	7 ± 2	7 ± 1	10 ± 2	8 ± 1	8 ± 2
MARHE [kW m^{-2}]	172 ± 5	174 ± 10	124 ± 11	155 ± 4	179 ± 10	178 ± 4	120 ± 12	151 ± 8
HRR_{max} [kW m^{-2}]	287 ± 41	267 ± 9	199 ± 20	256 ± 12	282 ± 30	296 ± 7	198 ± 14	267 ± 20
THR [MJ m^{-2}]	129 ± 4	133 ± 6	107 ± 9	115 ± 2	137 ± 9	129 ± 1	81 ± 4	93 ± 4
EHC [MJ kg^{-1}]	15.9 ± 0.6	16.0 ± 0.3	14.4 ± 1.4	14.6 ± 0.4	16.0 ± 1.2	14.7 ± 0.2	10.7 ± 0.7	12.3 ± 0.5
RM [%]	4.8 ± 1.1	4.5 ± 0.4	18.5 ± 1.2	11.1 ± 1.2	17.5 ± 1.5	15.3 ± 0.8	32.7 ± 0.7	30.6 ± 0.3
TSP [m^2 m^{-2}]	793 ± 17	740 ± 35	350 ± 79	680 ± 67	673 ± 119	774 ± 47	213 ± 42	209 ± 26
TCOP [g m^{-2}]	463 ± 28	391 ± 30	253 ± 36	267 ± 22	272 ± 36	264 ± 39	337 ± 22	315 ± 41
COY [g kg^{-1}]	57.1 ± 4.0	47.1 ± 1.1	34.0 ± 5.4	33.9 ± 2.4	31.7 ± 3.9	30.1 ± 4.2	44.5 ± 3.7	41.8 ± 6.2

TTI: time to ignition, MARHE: maximum average rate of heat emission, HRR_{max}: maximum value of heat release rate during the test, THR: total heat release, EHC: effective heat of combustion, RM: residual mass, TSP: total smoke production, TCOP: total carbon monoxide production, COY: carbon monoxide yield.

The time to ignition (TTI) was not significantly affected by any of the treatments, remaining consistent at approximately 7-8 seconds for most non-leached samples. This suggests the flame retardants act primarily during the combustion phase rather than delaying the initial ignition.

The raw wood samples served as a baseline for comparison. As expected, RW exhibited poor fire performance, characterized by a high MARHE of 172 kW m^{-2} and a high THR of 129 MJ m^{-2}. The combustion process left a minimal RM of only 4.8%. The leaching process had a negligible impact on the fire performance of raw wood, with all key metrics remaining statistically similar after leaching.

Before leaching, the AMP-W samples showed a significant improvement in fire retardancy compared to RW. The MARHE was reduced by 28% to 124 kW m^{-2}, and the RM increased nearly four-fold to 18.5%. This demonstrates the effectiveness of AMP in promoting char formation. However, this protective effect was almost completely lost after leaching. The MARHE of the leached AMP-W sample rose to 155 kW m^{-2}, nearly reverting to the level of raw wood, and the RM dropped to 11.1%. This performance collapse is directly explained by the poor leach retention of AMP (only 35.6%), confirming that the flame retardant was washed out of the wood matrix. The thermogravimetric analysis (TGA) further supports this, showing the thermal decomposition curve of leached AMP-W is nearly identical to that of RW.

The FA treatment, both before and after leaching, did not significantly improve the primary fire performance indicators such as MARHE or HRR_{max} compared to RW. However, it did notably increase the RM to 17.5% before leaching and 15.3% after, indicating that the polymerized FA network contributes to char formation. Crucially, the fire performance of FA-W was highly durable, with minimal changes to key metrics after the leaching process. This stability is attributed to the excellent leach retention of the in-situ polymerized FA (98.5%), which forms a stable, water-resistant matrix within the wood structure.

The combined FA+AMP (catalysed by H_3PO_4) treatment demonstrated a powerful synergistic effect, resulting in the best overall fire performance, which remained remarkably durable even after leaching. The non-leached FA+AMP-W samples showed outstanding fire retardancy. They achieved the lowest MARHE (120 kW m^{-2}) and THR (81 MJ m^{-2}) of all samples, representing a 30% and 37% reduction compared to RW, respectively. Most impressively, it produced the highest RM at 32.7%, a nearly seven-fold increase over RW, confirming a superior char-forming capability. The treatment was also highly effective at mitigating secondary fire hazards, significantly reducing TSP by 73% and COY by 22% compared to RW. While the leaching process slightly diminished its effectiveness, the leached FA+AMP-W samples still significantly outperformed all other samples, including non-leached RW. Compared to the leached RW control, the leached FA+AMP-W sample achieved a 30% reduction in THR (from 133 to 93 MJ m^{-2}), a 13% reduction in the MARHE, a 72% reduction in TSP, and a nearly seven-fold increase in RM, from 4.5% to over 30.6%.

The notable reduction in TSP and COY can be attributed to the synergistic condensed- and gas-phase flame-retardant mechanisms introduced by the phosphate/nitrogen system. Phosphoric acid species promote dehydration and carbonization of cellulose, yielding a stable and cohesive char layer that inhibits the release of volatile combustibles and soot precursors, thereby lowering smoke formation in the condensed phase. Concurrently, the thermal decomposition of ammonium-based moieties generates non-flammable gases (NH_3 and H_2O), which dilute combustible pyrolysis vapours and quench flame-propagating radicals in the gas phase, leading to more complete combustion and correspondingly lower CO and smoke yields. Similar dual-mechanism suppression of heat release and smoke emission has been reported for phosphorylated polysaccharides and bio-based intumescent flame-retardant systems in wood and transparent-wood composites (Fang et al. 2025; Guo et al. 2025a, b).

Fig. **10** provides a dynamic visualization of the fire behaviour of the different wood samples over time, complementing the summary data in Table 4. The graphs for Heat Release Rate (HRR), Total Heat Release (THR), CO production and smoke production rates clearly demonstrate the superior and durable performance of the combined FA+AMP (catalysed by H_3PO_4) treatment as it creates a highly effective flame-retardant system. It excels at reducing the main fire hazards—heat, smoke, and toxic gases—and, most importantly, retains this high level of performance after being subjected to a rigorous leaching procedure.

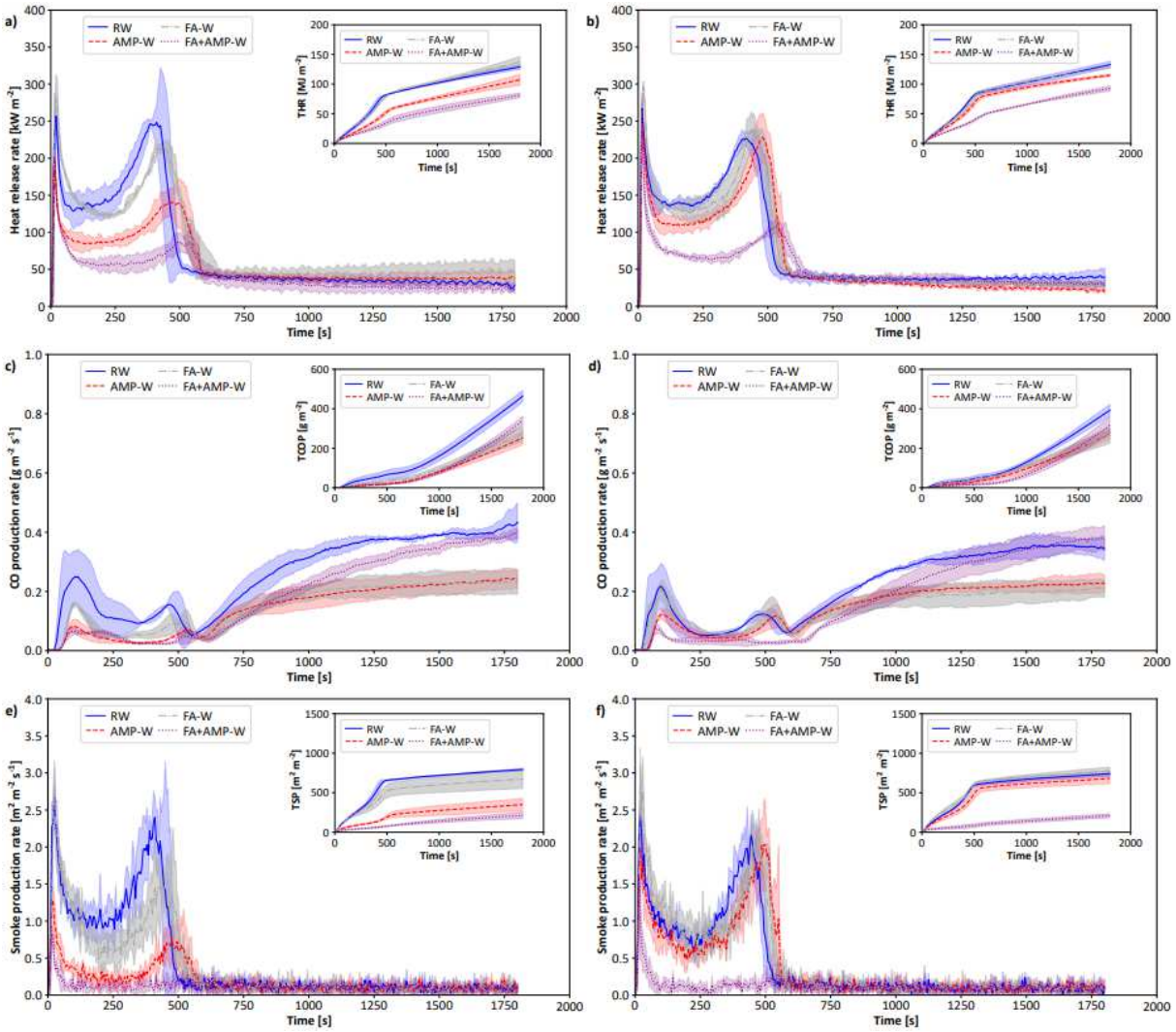

Fig. 10. Time-dependent fire performance of wood samples from cone calorimeter tests, comparing raw wood (RW), furfuryl alcohol-treated wood (FA-W), ammonium phytate-treated wood (AMP-W), and the combined treatment (FA+AMP-W). The figure shows: (a, b) Heat Release Rate (HRR) and inset Total Heat Release (THR); (c, d) Carbon Monoxide (CO) production rate and inset Total CO Production; and (e, f) Smoke production rate and inset Total Smoke Production (TSP). The left column (a, c, e) presents data for samples before leaching, while the right column (b, d, f) shows data after the leaching procedure. Solid lines depict the mean values, with the standard deviations represented by the shaded regions.

Comparison of obtained results with performance of flame retardants (for woods) reported by Lee et al., suggests that FA+AMP-W reaches level of high-end flame retardants (for woods) even after leaching (Lee et al. 2025). This exceptional durability is a direct result of the furfuryl alcohol polymer matrix effectively entrapping and fixing the AMP flame retardant within the wood, as evidenced by the high leach retention of 91.5%. The synergistic mechanism involves AMP's nitrogen-phosphorus action promoting a dense, insulating char layer (Qin et al. 2023), while the stable FA network ensures the flame retardant remains in place to function effectively, even after prolonged water exposure (Lin et al. 2021b). This combined action is the key to creating a durable, high-performance, flame-retardant lignocellulosic material. The

main flame-retardant effect of phosphoric acid is the support of char layer formation (Kim and Kim 2025).

Limiting oxygen index

Raw wood (RW) exhibits the lowest LOI value at 18%, which is typical for untreated lignocellulosic materials and indicates high flammability. Treatment with ammonium phytate alone (AMP-W) increases the LOI to 26%, reflecting the known flame-retardant effect of phosphorus-based additives. Ammonium phytate functions primarily through a condensed-phase mechanism, promoting char formation and reducing the release of flammable volatiles during combustion (Qin et al., 2023).

In contrast, furfuryl alcohol treatment alone (FA-W) leads to a modest LOI increase to 21%. Although FA does not act as a flame retardant per se, its polymerization within the wood cell walls results in a denser, more thermally stable structure, which likely slows degradation and ignition. This moderate increase supports the idea that FA contributes indirectly to fire resistance through structural modification and enhanced thermal insulation (Esteves and Pereira, 2008).

The highest LOI (28%) is observed for the combined FA+AMP-W treatment, indicating a clear synergistic effect between furfuryl alcohol and ammonium phytate. The improved retention of AMP due to the presence of FA (as shown previously) ensures that the phosphorus-based flame retardant remains in the matrix during combustion. Simultaneously, the furfurylated structure enhances the thermal stability and promotes char formation. Together, these effects suppress flaming combustion and increase the oxygen concentration required to sustain burning. Such synergistic improvements are consistent with other studies where the incorporation of phosphorus compounds within crosslinked polymer matrices significantly boosts flame-retardant efficacy (C. Lin et al., 2021; Ni et al., 2024).The Limiting Oxygen Index (LOI) results presented in Fig. **11** demonstrate significant improvements in flame retardancy as a result of chemical modification.

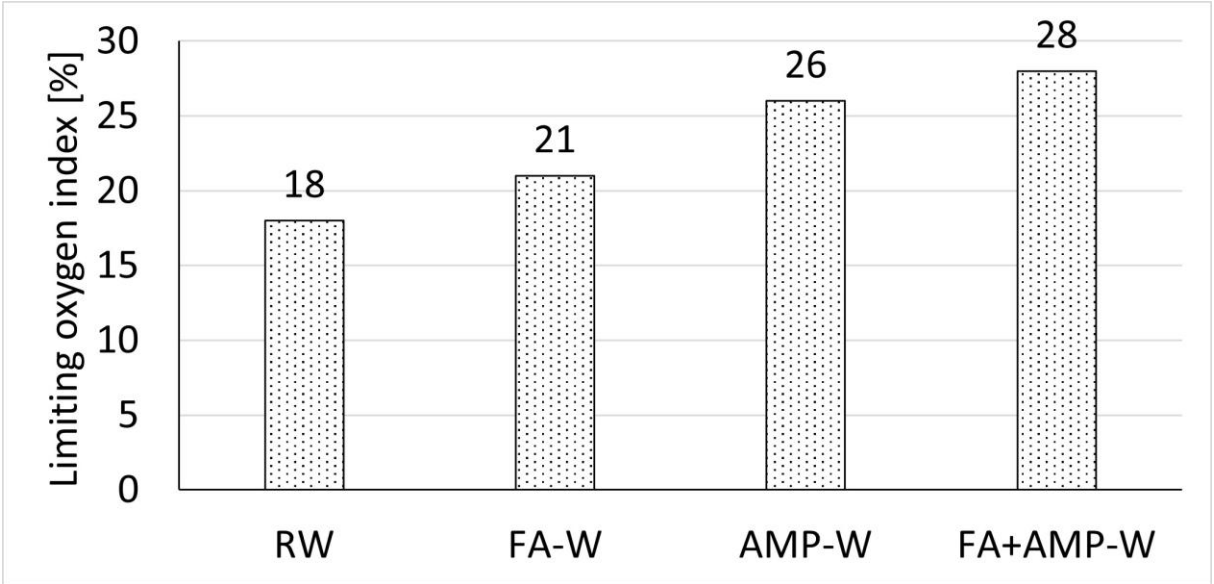

Fig. 11. Limiting Oxygen Index (LOI) of raw wood (RW); ammonium phytate-treated wood (AMP-W); furfuryl alcohol-treated wood (FA-W); and furfuryl alcohol and ammonium phytate-treated wood (FA+AMP-W).

Duncan's Multiple Range Test is not applicable to LOI data due to the threshold-based nature of the LOI measurement.

Flame test

To evaluate the flame retardancy of the modified wood samples, a propane torch flame test was conducted. The ignition behaviour and subsequent combustion characteristics were documented (Fig. 12). When subjected to the flame, raw wood (RW) demonstrated immediate ignition and rapid flame spread. Following a 10-second exposure, the entire wood block underwent vigorous combustion, culminating in complete burning within 65 seconds.

Unlike the rapid ignition and continuous burning seen in RW, AMP treated wood (AMP-W) showed a clear decrease in flame size after being exposed to a flame for 10 seconds, and it stopped burning on its own within another 37 seconds. This improved resistance to fire results from a combination of processes happening in both the gas and solid phases. When burning, AMP breaks down due to heat, releasing gases that don't burn, like ammonia and water vapor, which reduce the amount of oxygen available, thus suppressing the fire. Additionally, the volatile products produced during this breakdown include small molecules that act as scavengers of free radicals, interrupting the chemical reactions that keep a flame going. At the same time, the phosphoric acid that is released as AMP decomposes acts as a dehydrating agent, helping to form a protective layer of char from the wood's components and the PFA. The nitrogen contained within AMP also plays a role in building this dense char layer, which further enhances the material's ability to resist fire.

The furfuryl alcohol treated wood (FA-W) exhibited similar characteristic behaviour to RW. After removing the test flame the whole wood surface was engulfed with flames accompanied by a significant crackling and pieces of wood flying off the samples. While complete combustion occurred within 79 seconds, the FA-treated wood yielded a substantially greater amount of residual char compared to untreated wood.

Unlike the previous observations, or the FA+AMP-treated wood, self-extinguishment occurred remarkably quickly, within 9 seconds after the flame removal. This rapid response highlights the synergistic flame-retardant effect between AMP and polymerized FA. AMP, through its nitrogen-phosphorus intumescent mechanism, and FA, by promoting char formation, work together to create a dense char layer. By creating a barrier, this layer limits heat transfer, the release of combustible gases, and the entry of oxygen. As a result, it drastically lowers the intensity of combustion and emissions. The combined action of these components substantially enhances the wood's flame retardancy.

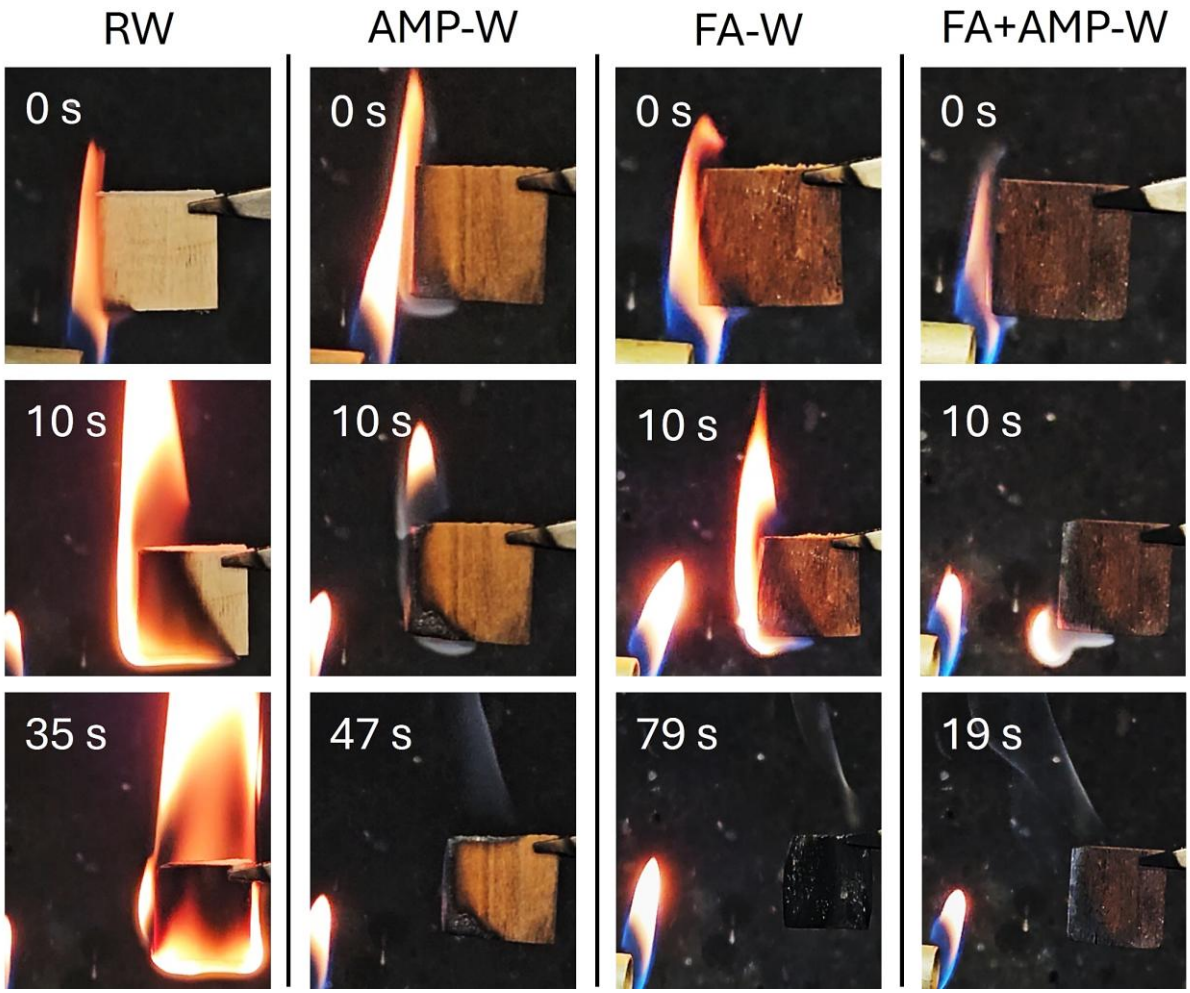

Fig. 12. Flame test progression of various wood samples. The rows display the temporal stages of the test: 0 s (test flame application), 10 s (test flame removal), and flame extinction (except RW, where a fully developed flame is displayed). The columns correspond to the following wood treatments: raw wood (RW); ammonium phytate-treated wood (AMP-W); furfuryl alcohol-treated wood (FA-W); furfuryl alcohol and ammonium phytate-treated wood (FA+AMP-W)

While previous studies have investigated furfuryl alcohol (FA) in combination with phosphorus-based flame retardants, our work advances this concept in several critical ways. Kong et al., (2018) demonstrated improvements in dimensional stability and fire performance of poplar by combining FA with ammonium dihydrogen phosphate; however, the high loading levels and the inorganic phosphate used resulted in limited leach resistance. More recently, Xie et al., (2024) reported the use of FA with ammonium phytate (AMP), yet their system required higher concentrations of reagents and did not fully address the durability of flame-retardant performance after leaching. In contrast, the present study employs lower concentrations of both FA (15 wt%) and AMP (4 wt%), while introducing phosphoric acid as a catalyst, which not only promotes in-situ polymerization of FA but also contributes additional phosphorus to the system, enhancing char formation. This approach achieved a >91% leach resistance, ensuring long-term stability of the fire-retardant effect. Moreover, our work uniquely provides a comprehensive evaluation of fire and mechanical performance both

before and after leaching, demonstrating that the synergistic FA–AMP–H_3PO_4 system maintains high flame retardancy.

CONCLUSION

A fully bio-based flame retardant was developed for poplar wood using an in-situ polymerization process combining furfuryl alcohol (FA) and ammonium phytate (AMP). Catalysed by phosphoric acid, this method effectively immobilized AMP, achieving a weight percent gain of 21.7% and leach resistance over 91%.
The multifunctional performance of the treated wood was outstanding. Fire resistance improved substantially: the limiting oxygen index (LOI) increased from 18% to 28%, the total heat release decreased by 37% (from 129 to 81 MJ m^{-2}), smoke production was reduced by 73%, and the residual mass rose from 4.8% to 32.7%. In direct flame tests, FA+AMP-W self-extinguished within 9 seconds, whereas RW burned completely in 65 seconds. Crucially, these properties were retained after leaching, confirming long-term durability. These findings highlight that the dual condensed- and gas-phase mechanisms jointly reduce smoke and CO emissions, resulting in improved fire performance.

Beyond confirming the synergistic nitrogen–phosphorus intumescent action of AMP and the structural reinforcement provided by FA, this work presents one of the first demonstrations of a bio-based, leach-resistant flame-retardant treatment for poplar wood. By using relatively low concentrations of AMP (4 wt%) and FA (15 wt%), catalysed by phosphoric acid, this system achieves durable fixation of the flame retardant while incorporating additional phosphorus into the matrix, delivering exceptional fire resistance and mechanical performance even after water exposure.

Overall, this strategy establishes a viable, eco-friendly pathway to transform low-cost poplar into a high-performance, fire-safe, and durable material suitable for structural, decorative, and interior applications. Future research should address long-term outdoor weathering, scale-up of the impregnation process, and life-cycle environmental assessment to validate industrial use. If successfully developed, this approach could enable safer, higher-value applications of poplar wood in construction, furniture, and interior design, while reducing reliance on unsustainable chemical fire retardants.

RESEARCH FUNDING

Funded by the EU NextGenerationEU through the Recovery and Resilience Plan for Slovakia under the project No. 09I03-03-V04-00459

REFERENCES

Abou-okeil A, El-Sawy S, Abdel-Mohdy FA (2013) Flame retardant cotton fabrics treated with organophosphorus polymer. Carbohydr Polym 92:2293–2298. https://doi.org/10.1016/j.carbpol.2012.12.008

Acosta AP, Beltrame R, Missio AL, et al (2022) Juvenile and mature woods from pine subjected

698 to in situ polymerization with furfuryl alcohol. Wood Mater Sci Eng 17:151–156.
699 https://doi.org/10.1080/17480272.2020.1810118
700 Brisebois P, Aouinti M, Jafari M, et al (2025) Adsorption Dynamics of Disodium Octaborate
701 Tetrahydrate on Clay Minerals: Implications for Construction Wood Protection. Small
702 Methods 9:2400753. https://doi.org/https://doi.org/10.1002/smtd.202400753
703 Candan Z, Korkut S, ÜNSAL Ö (2013) Thermally Compressed Poplar Wood (TCW): Physical and
704 Mechanical Properties. Drv Ind 64:. https://doi.org/10.5552/drind.2013.1216
705 Cheng X-W, Guan J-P, Tang R-C, Liu K-Q (2016) Phytic acid as a bio-based phosphorus flame
706 retardant for poly(lactic acid) nonwoven fabric. J Clean Prod 124:114–119.
707 https://doi.org/https://doi.org/10.1016/j.jclepro.2016.02.113
708 Dong Y, Xue Q, Fu Z, et al (2023) Enhancing wood stability and fire retardancy through citric
709 acid and phosphorylated sucrose stearate cross-linking modification. Constr Build Mater
710 393:131946. https://doi.org/https://doi.org/10.1016/j.conbuildmat.2023.131946
711 Ehmcke G, Koch G, Richter K, Pilgård A (2020) Topochemical and light microscopic
712 investigations of non-enzymatic oxidative changes at the initial decay stage of furfuryl
713 alcohol-modified radiata pine (Pinus radiata) degraded by the brown rot fungus Rhodonia
714 placenta. Int Biodeterior Biodegradation 154:105020.
715 https://doi.org/https://doi.org/10.1016/j.ibiod.2020.105020
716 Fang Y, Chen K, Xu L, et al (2025) Advances in Wood Processing, Flame-Retardant
717 Functionalization, and Multifunctional Applications. Polymers (Basel). 17
718 Fang Y, Wu J, Sun W, Liu X (2022) Pyrolysis of Precious Chinese Xuan Paper Containing
719 Ammonium Phytate as a Flame Retardant. ACS Omega 7:37971–37979.
720 https://doi.org/10.1021/acsomega.2c05138
721 Feng Y, Zhou Y, Li D, et al (2017) A plant-based reactive ammonium phytate for use as a flame-
722 retardant for cotton fabric. Carbohydr Polym 175:636–644.
723 https://doi.org/https://doi.org/10.1016/j.carbpol.2017.06.129
724 Gaefke C, Botelho E, Ferreira N, Rezende MC (2007) Effect of furfuryl alcohol addition on the
725 cure of furfuryl alcohol resin used in the glassy carbon manufacture. J Appl Polym Sci
726 106:2274–2281. https://doi.org/10.1002/app.26938
727 Gao Y-Y, Deng C, Du Y-Y, et al (2019) A novel bio-based flame retardant for polypropylene from
728 phytic acid. Polym Degrad Stab 161:.
729 https://doi.org/10.1016/j.polymdegradstab.2019.02.005
730 Guo M, Pan Y, Xu S, et al (2025a) Phosphorylated sodium alginate-filled delignified wood-
731 reinforced transparent wood: Crafting flame-retardant composites. Carbohydr Polym
732 366:124021. https://doi.org/https://doi.org/10.1016/j.carbpol.2025.124021
733 Guo M, Pan Y, Xu S, et al (2025b) Sustainable, transparent and fire-retardant wood
734 composites. Ind Crops Prod 233:121332.
735 https://doi.org/https://doi.org/10.1016/j.indcrop.2025.121332
736 Hörold S (2014) Chapter 6 - Phosphorus-based and Intumescent Flame Retardants. In:
737 Papaspyrides CD, Kiliaris PBT-PGFR (eds). Elsevier, Amsterdam, pp 221–254
738 International Organization for Standardization (2015) ISO 5660-1:2015 Reaction-to-fire tests
739 — Heat release, smoke production and mass loss rate — Part 1: Heat release rate (cone
740 calorimeter method) and smoke production rate (dynamic measurement). 55
741 International Organization for Standardization (2017) Plastics — Determination of the burning
742 behaviour by oxygen index — Part 2: Ambient-temperature test (ISO Standard No. 4589-
743 2:2017)
744 Iroegbu AOC, Ray SS (2024) On the chemistry of furfuryl alcohol polymerization: A review. J

745 Polym Sci 62:1044–1060. https://doi.org/https://doi.org/10.1002/pol.20230708
746 Jones D, Sandberg D, Goli G, Todaro L (2020) Wood Modification in Europe: a state-of-the-art
747 about processes, products and applications
748 Kim G, Kim D (2025) The Effect of Phosphoric Acid on the Flame Retardancy and Interfacial
749 Adhesion of Carbon Fiber with Thermoplastic Resin PA6. Polymers (Basel). 17
750 Kong L, Guan H, Wang X (2018) In Situ Polymerization of Furfuryl Alcohol with Ammonium
751 Dihydrogen Phosphate in Poplar Wood for Improved Dimensional Stability and Flame
752 Retardancy. ACS Sustain Chem Eng 6:3349–3357.
753 https://doi.org/10.1021/acssuschemeng.7b03518
754 Lee YX, Wang W, Lei Y, et al (2025) Flame-retardant coatings for wooden structures. Prog Org
755 Coatings 198:108903. https://doi.org/https://doi.org/10.1016/j.porgcoat.2024.108903
756 Li H, Zheng Z, Liu Y, et al (2024) Construction of fully bio-based flame retardant and
757 antibacterial coating on polyester fabric with chitosan and ammonium phytate. J Appl
758 Polym Sci 141:. https://doi.org/10.1002/app.55940
759 Li J, Jiang W, Liu M (2022) Durable phosphorus/nitrogen flame retardant for cotton fabric.
760 Cellulose 29:4725–4751. https://doi.org/10.1007/s10570-022-04558-x
761 Li L, Yu L, Wu Z, Hu Y (2019) Delignification of poplar wood with lactic acid-based deep eutectic
762 solvents. Wood Res 64:507–522
763 Lin C-F, Karlsson O, Martinka J, et al (2021a) Approaching Highly Leaching-Resistant Fire-
764 Retardant Wood by In Situ Polymerization with Melamine Formaldehyde Resin. ACS
765 omega 6:12733–12745. https://doi.org/10.1021/acsomega.1c01044
766 Lin C, Kim I, Mantanis GI, et al (2021b) Leach-resistant fire-retardant treated furfurylated wood
767 by incorporating guanyl-urea phosphate. Wood Mater Sci Eng 16:429–431.
768 https://doi.org/10.1080/17480272.2021.1981998
769 Liu Q, Du H, Lyu W (2021) Physical and Mechanical Properties of Poplar Wood Modified by
770 Glucose-Urea-Melamine Resin/Sodium Silicate Compound. Forests 12:127.
771 https://doi.org/10.3390/f12020127
772 Liu X, Liu J, Dong Y, et al (2022) Evaluation of natural weathering and thermal degradation
773 behavior of furfurylated bamboo strips at different weight percent gain. Eur J Wood
774 Wood Prod 80:289–299. https://doi.org/10.1007/s00107-021-01784-1
775 Liu X, Zhang Q, Cheng B, et al (2018) Durable flame retardant cellulosic fibers modified with
776 novel, facile and efficient phytic acid-based finishing agent. Cellulose 25:799–811
777 Lowden LA, Hull TR (2013) Flammability behaviour of wood and a review of the methods for
778 its reduction. Fire Sci Rev 2:4. https://doi.org/10.1186/2193-0414-2-4
779 Mubarok M, Azadeh E, Obounou Akong F, et al (2023) Effect of Tannins Addition on Thermal
780 Stability of Furfurylated Wood. Polymers (Basel). 15
781 Ni M, Li L, Wu Y, et al (2024) Biobased Furfurylated Poplar Wood for Flame-Retardant
782 Modification with Boric Acid and Ammonium Dihydrogen Phosphate. J. Renew. Mater.
783 12
784 Page J, Whaley P, Bellingham M, et al (2023) A new consensus on reconciling fire safety with
785 environmental & health impacts of chemical flame retardants. Environ Int 173:107782.
786 https://doi.org/https://doi.org/10.1016/j.envint.2023.107782
787 Qin S, Liu Y, Shi X, et al (2023) Phytic acid-based NP fire retardant and its effect on combustion
788 property of poplar wood. BioResources 19:955–972.
789 https://doi.org/10.15376/biores.19.1.955-972
790 Rowell R (1983) Chemical Modification of Wood. For Prod Abstr 6:.
791 https://doi.org/10.3139/9783446442504.022

Rowell R (2005) Handbook Of Wood Chemistry And Wood Composites
Sangregorio A, Muralidhara A, Guigo N, et al (2020) Humin based resin for wood modification and property improvement. Green Chem 22:2786–2798. https://doi.org/10.1039/C9GC03620B
Song F, Liu T, Fan Q, et al (2022) Sustainable, high-performance, flame-retardant waterborne wood coatings via phytic acid based green curing agent for melamine-urea-formaldehyde resin. Prog Org Coatings 162:106597. https://doi.org/https://doi.org/10.1016/j.porgcoat.2021.106597
Sun H, Chang X, Fu C, et al (2022) Effect of Impregnation with a Low-Concentration Furfuryl Alcohol Aqueous Solution on Hygroscopic Properties of Chinese Fir and Poplar Wood. Forests 13
Thygesen L, Thybring E, Hoffmeyer P (2010) Water sorption in wood and modified wood at high values of relative humidity. Part I: Results for untreated, acetylated, and furfurylated Norway spruce. Holzforschung 64:315–323. https://doi.org/10.1515/HF.2010.044
Vahedi N, Tiago C, Vassilopoulos AP, et al (2022) Thermophysical properties of balsa wood used as core of sandwich composite bridge decks exposed to external fire. Constr Build Mater 329:127164. https://doi.org/https://doi.org/10.1016/j.conbuildmat.2022.127164
Wu M, Emmerich L, Kurkowiak K, Militz H (2023) Fire resistance of pine wood treated with phenol-formaldehyde resin and phosphate-based flame retardant. Wood Mater Sci Eng 18:1933–1939. https://doi.org/10.1080/17480272.2023.2205379
Xie K, Gao A, Zhang Y (2013) Flame retardant finishing of cotton fabric based on synergistic compounds containing boron and nitrogen. Carbohydr Polym 98:706–710. https://doi.org/10.1016/j.carbpol.2013.06.014
Xie S, Liu Z, Feng A, et al (2024) Flame retardant modification of poplar wood based on sustainable impregnation solution with high biomass content. Ind Crops Prod 215:118616. https://doi.org/https://doi.org/10.1016/j.indcrop.2024.118616
Yang T, Mei C, Ma E (2022a) Combined effects of multi-interfacial furfurylation and densification on mechanical-physical performances of fast-growing poplar wood. J Mater Sci 57:15340–15353. https://doi.org/10.1007/s10853-022-07581-2
Yang T, Zhang K, Mei C, et al (2022b) Effects of furfurylation on interactions between moisture sorption and humidity conditioning of wood. Wood Sci Technol 56:703–720. https://doi.org/10.1007/s00226-022-01375-0
Yao M, Yang Y, Song J, et al (2017) Lignin-based catalysts for Chinese fir furfurylation to improve dimensional stability and mechanical properties. Ind Crops Prod 107:38–44. https://doi.org/https://doi.org/10.1016/j.indcrop.2017.05.038
Zhang L, Chen K, Xu B, et al (2022a) Parallel-to-Grain Compressive and Tensile Behavior of Paulownia Wood at Elevated Temperatures. Appl. Sci. 12
Zhang L, Xu J, Shen H, et al (2021) Montmorillonite-catalyzed furfurylated wood for flame retardancy. Fire Saf J 121:103297. https://doi.org/https://doi.org/10.1016/j.firesaf.2021.103297
Zhang L, Zhang W, Peng Y, et al (2022b) Thermal behavior and flame retardancy of poplar wood impregnated with furfuryl alcohol catalyzed by boron/phosphorus compound system. Ind Crops Prod 176:114361. https://doi.org/https://doi.org/10.1016/j.indcrop.2021.114361
Zhang S, Chen Z, Ding M, et al (2020) Reducing the fire toxicity of wood composites using hierarchically porous 4A (H4A) zeolite modified ammonium polyphosphate (APP) synthesized by a facile in-situ method. Constr Build Mater 262:120754.

https://doi.org/https://doi.org/10.1016/j.conbuildmat.2020.120754
Zhang S, Yang W, Yang T, et al (2023) Thermal degradation, flame retardancy, and char analysis of ammonium phytate-based flame retardant treated loblolly pine wood. Eur J Wood Wood Prod 81:957–971. https://doi.org/10.1007/s00107-023-01927-6
Zhou Q, Chen C, Tu D, et al (2019) Surface densification of poplar solid wood: Effects of the process parameters on the density profile and hardness. BioResources 14:4814–4831. https://doi.org/10.15376/biores.14.2.4814-4831
Zuo C, Guo Y, Jiang L, et al (2023) Fabrication of durable flame retardant PAN fibers through bio-based ammonium phytate surface modification and highly efficient thermal oxidation. Eur Polym J 196:112304. https://doi.org/https://doi.org/10.1016/j.eurpolymj.2023.112304

Supplementary Files

This is a list of supplementary files associated with this preprint. Click to download.

- SupplementarymaterialA.docx